

Micrometer-scale magnetometry of thin $\text{Ni}_{80}\text{Fe}_{20}$ films using ultrasensitive microcantilevers

Michelle D. Chabot^{a)} and John Moreland

National Institute of Standards and Technology, Boulder, Colorado 80305

(Presented on 14 November 2002)

Microcantilever torque magnetometry is used to measure quantitative M - H curves on patterned $\text{Ni}_{80}\text{Fe}_{20}$ films. The dynamic deflection method is employed, in which a small film is deposited onto a microcantilever and placed in an external magnetic field. A small orthogonal ac torque field is applied at the cantilever's resonant frequency, and the resulting torque is measured as a function of external field. Film patterning and deposition have been integrated with cantilever fabrication. Results are presented for a $5\ \mu\text{m} \times 5\ \mu\text{m} \times 30\ \mu\text{m}$ Ni-Fe film. The measured saturated magnetic moment of the sample is $5.1 \pm 0.2 \times 10^{-13}\ \text{A m}^2$ for a $100\ \text{A/m}$ torque field. The M - H curves for the smaller films show hysteretic switching consistent with a series of stable multi-domain states. Values of the saturation magnetization are within 3% of the value measured on similar samples by ferromagnetic resonance, indicating this is a sensitive method for measuring magnetic reversal in small ferromagnetic samples. [DOI: 10.1063/1.1557759]

Micrometer and submicrometer scale magnetic measurements have proven to be a challenge for conventional magnetometers, and new methods are being employed to probe magnetism on this scale. Currently, many measurements are made on arrays of micromagnetic dots.¹ However, due to fabrication limitations, these results are clouded by statistical variations within the array such as dot shape, size, and spacing. Thus, more sensitive detectors are needed that can measure magnetic properties on individual particles. Recently, various methods have been used to probe individual or isolated samples, including magnetic force microscopy,² magnetoresistance measurements,³ magneto-optics,⁴ Lorentz microscopy,⁵ superconducting quantum interference device magnetometry,⁶ and microcantilever torque magnetometry.⁷⁻¹¹

Of these, microcantilever torque magnetometry has the most diverse measurement methods, all of which have their pros and cons. Measurement of the frequency shift and dissipation as a function of applied field⁷⁻⁹ (referred to as the dynamic mode of operation) yields the best resolution but requires a model of the magnetization in order to extract quantitative information above the sample's magnetic properties. The static mode of operation uses the torque created between the applied field and the magnetization to cause a measurable deflection of the cantilever,⁸ but this method does not operate at the cantilever's resonance and therefore sacrifices sensitivity. Another method is the dynamic equivalent of the static mode but employs a small alternating torque field orthogonal to the applied field, resulting in torsional excitation of the cantilever.^{10,11} This dynamic deflection method offers the advantage of higher sensitivities due to

resonant enhancement and also enables direct measurements of the magnetization to be made without the need for a model to fit the data.

Regardless of which microcantilever magnetometry method is used, a main challenge of this measurement technique is obtaining well-defined micromagnetic samples on cantilevers. To this end, we have created a process in which patterning and deposition of the film are combined with the cantilever fabrication process. In this article we present cantilever magnetometry results on these microfabricated patterned $\text{Ni}_{80}\text{Fe}_{20}$ films with dimensions as small as $5\ \mu\text{m} \times 5\ \mu\text{m} \times 30\ \text{nm}$.

Figure 1 shows the experimental setup. A small Ni-Fe film is deposited onto a mechanical oscillator and placed in an external magnetic field, H_0 . The field is applied in the plane of the film and perpendicular to the axis of the cantilever. It is created by an iron core electromagnet that can be ramped from $+50$ to $-20\ \text{kA/m}$, with the offset due to a small permanent magnet used to eliminate artificial noise caused by switching the current polarity. A small torque field ($H_T = 15$ – $100\ \text{A/m}$) is applied perpendicular to the plane of the film. H_T is varied at the resonant frequency of the cantilever.

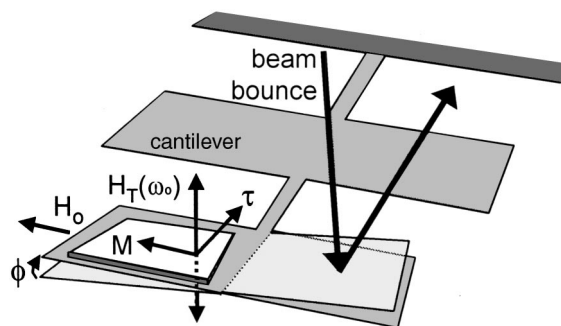


FIG. 1. Experimental setup for cantilever magnetometry using the dynamic deflection mode of operation and a torsional oscillator.

^{a)} Author to whom correspondence should be addressed; electronic mail: chabot@boulder.nist.gov

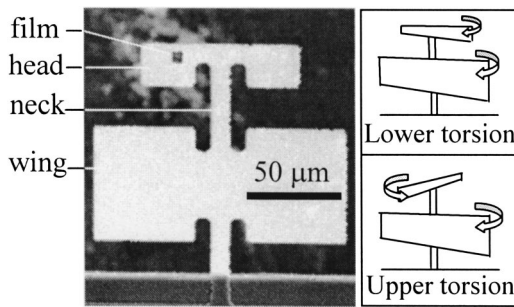


FIG. 2. Scanning electron micrograph of a single-crystal silicon torsional oscillator with the $5\ \mu\text{m}\times 5\ \mu\text{m}\times 30\ \text{nm}$ Ni-Fe film used in this work. Upper and lower torsional modes are illustrated on the right.

lever ω_0 , resulting in an oscillating torque given by

$$\tau(\omega_0) = \mu_0 |M \times H_T(\omega_0)| V = \mu_0 M H_T(\omega_0) V, \quad (1)$$

where V is the volume of the film, and the angle between M and H_T is assumed to be 90° . If the rotation of the magnetization out of plane is less than 5° , the in-plane magnetization is within 1% of its value at $H_T=0$, and Eq. (1) is valid. The in-plane and out-of-plane anisotropy fields for a given material and geometry determine the field strength necessary to rotate the magnetization by 5° out of plane. For the 30-nm-thick Ni-Fe films used in this work, shape anisotropy is the dominating factor, and torque fields on the order of 700 kA/m are required to rotate the magnetization by 5° .¹² Therefore, since the values of H_T are all less than 100 A/m, Eq. (1) is a valid approximation.

The amplitude of oscillation is detected with an atomic force microscope head with a beam-bounce detection system. A four-quadrant photodiode allows for the torsion and deflection modes to be separated. The measured voltage is converted to a cantilever rotation angle ϕ by use of the calibration factor: $1\ \text{V} = 7.64 \times 10^{-4}$ rad. The measured value for ϕ is then converted to a torque using $\tau = \kappa\phi/Q$, where κ is the torsional spring constant of the oscillator and Q is the quality factor. It is assumed that the measurement was made while operating on resonance.

The sensitivity of this cantilever magnetometry method is limited by the thermal noise of the mechanical oscillator. Therefore high sensitivity is obtained by operating in vacuum and by fabricating oscillators that have low κ , high Q , and high ω_0 . Single-crystal silicon multiple-torsional oscillators^{13,14} were fabricated for use in this work. The multiple-torsional oscillator geometry (Fig. 2) offers the advantage of an upper torsional mode of operation that has a higher Q and a higher resonant frequency than the lower torsional mode. The higher Q arises because most of the energy of oscillation is stored in the head, which is not directly coupled to the fixed base. These oscillators have been characterized at room temperature and a pressure of 13 Pa using magnetic excitation. For the lower torsional mode, we find an average $\omega_0 \approx 50$ kHz and $Q \approx 4000$. For the upper torsional mode, $\omega_0 \approx 120$ kHz, and $Q \approx 12\ 000$. From elastic theory, the torsional spring constant of the oscillator neck is

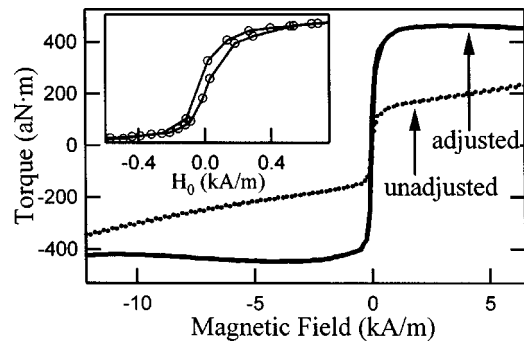


FIG. 3. Unadjusted (dashed line) and adjusted (solid line) M - H curves for a Ni-Fe film with $V = 3.6 \times 10^{-17}$ m³. Inset: Close-up view of adjusted loop showing hysteresis.

calculated to be¹⁵

$$\kappa = \frac{Ewt^3}{6l(1+n)}, \quad (2)$$

where E is Young's modulus ($E = 1.3 \times 10^{11}$ N/m²), n is the Poisson ratio ($n = 0.28$), l is the length, w is the width, and t is the thickness of the neck. Using $l = 35\ \mu\text{m}$, $w = 10\ \mu\text{m}$, and $t = 1\ \mu\text{m}$, we find $\kappa = 5 \times 10^{-9}$ N m.

As mentioned previously, a chief challenge of cantilever magnetometry is obtaining well-defined films on cantilevers. This obstacle has been overcome by integrating film patterning and deposition with oscillator fabrication. The magnetic film is deposited onto a silicon wafer that has been processed to create several boron-doped membranes that are coated with patterned photoresist. The resist is removed, leaving behind the patterned magnetic films on the thin membranes. A last patterning step is done in which parts of the membranes are etched away, leaving behind free-standing single-crystal silicon multiple-torsional oscillators with the films situated on their heads (Fig. 2). The Ni-Fe films are prepared by thermal evaporation at a pressure of 1.2×10^{-4} Pa and an evaporation rate of 0.5 nm/s.

Figure 3 shows the results obtained for a 30 nm film deposited onto the whole head of an oscillator, corresponding to a volume of 3.6×10^{-17} m³. The data were adjusted to compensate for the large resonant frequency shift that occurs with H_0 due to magnetic stiffening of the oscillator. This stiffening effect is plotted in Fig. 4, indicating an approximately linear shift of 0.91 Hz/(kA/m) for fields up to 50 kA/m. The M - H curve in Fig. 3 was measured for $H_T(\omega_0)$ oscillating at 49.220 kHz, which corresponds to the cantilever being tuned at $H_0 = 14$ kA/m. As H_0 is ramped away from 14 kA/m, the amplitude decreases as a function of the

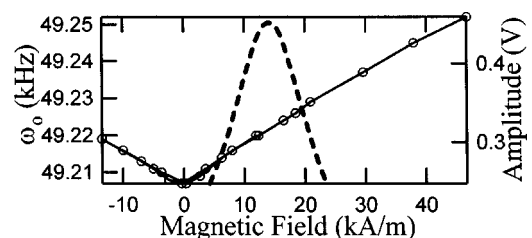


FIG. 4. Resonance frequency of oscillator (circles, left axis) vs applied field. Amplitude of oscillator tuned to 49 220 kHz (dashed line, right axis) vs field.

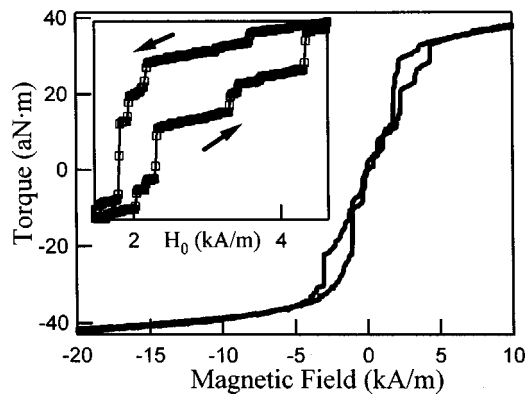


FIG. 5. Torque vs applied field for a $5\ \mu\text{m} \times 5\ \mu\text{m} \times 30\ \text{nm}$ Ni-Fe film. Inset: close-up of hysteresis showing domain switching.

Q of the oscillator. The resonance curve as a function of H_0 for the oscillator tuned to 49 200 kHz with a measured Q of 4000 is plotted in Fig. 4. The measured amplitude as a function of H_0 is multiplied by the ratio of the maximum amplitude of the resonance curve at 14 kA/m to the amplitude of the resonance curve for the particular field at which the measurement was taken. Both the adjusted and unadjusted data are shown in Fig. 3. The unadjusted curve shows an apparent increase after saturation that is not evident in the adjusted data, indicating that this effect is due solely to magnetic stiffening, as expected. It is also important to note that while frequency shift is caused by a change in the spring constant $\Delta\kappa$, this is insignificant to the calculation of the torque since $\Delta\kappa \approx 1 \times 10^{-13}\ \text{N m}/(\text{kA/m})$ and is therefore negligible compared to the zero-field value $5 \times 10^{-9}\ \text{N m}$.⁷

The 450 mV amplitude at saturation for the $3.6 \times 10^{-17}\ \text{m}^3$ film corresponds to a torque of $4.4 \times 10^{-16}\ \text{N m}$. The torque field is estimated to be 15 A/m, which yields a measured saturation magnetization of 650 kA/m. This is within 3% of measurements made on similar Ni-Fe films using ferromagnetic resonance (FMR), where M_s was found to be 670 kA/m.¹¹

Figure 5 shows the M - H curve from the $5\ \mu\text{m} \times 5\ \mu\text{m} \times 30\ \text{nm}$ ($7.5 \times 10^{-19}\ \text{m}^3$) Ni-Fe film shown in Fig. 2. The inset of Fig. 5 is a close-up of the hysteresis during switching, showing finite steps consistent with a series of stable multi-domain states. These steps were repeatable for different runs. Similar hysteretic switching behavior was observed in $7\ \mu\text{m} \times 7\ \mu\text{m} \times 30\ \text{nm}$ and $10\ \mu\text{m} \times 10\ \mu\text{m} \times 30\ \text{nm}$ films. The adjustment to compensate for the frequency shift was unnecessary since the measured frequency shift was only 1 Hz over the entire 40 kA/m range. The measured amplitude at saturation was 40 mV, corresponding to a torque of $4.2 \times 10^{-17}\ \text{N m}$. A torque field of approximately 65 A/m was used, which leads to a saturation magnetization of 685 kA/m, again in good agreement with the value measured by FMR on similar films.¹¹ The signal-to-noise ratio was 50 ± 5 ,

indicating a torque resolution of $8.4 \times 0.7 \times 10^{-19}\ \text{N m}$. For a torque field of 100 A/m, this corresponds to a moment sensitivity of $6.7 \times 10^{-15}\ \text{A m}^2$. This is consistent with the predicted thermal noise level of the cantilever.

These results indicate that the dynamic deflection mode of operation for microcantilever torque magnetometry is a reliable and sensitive way to make quantitative measurements on small ferromagnetic samples. Current moment sensitivity is $6.7 \times 10^{-15}\ \text{A m}^2 (7.2 \times 10^8\ \mu_B)$ for $H_T = 100\ \text{A/m}$. Measured values of the saturation magnetization of Ni-Fe are within 3% of previous values obtained by FMR, illustrating that this is indeed a feasible method for measuring quantitative M - H curves without modeling. The chief challenge of obtaining well-defined samples on microcantilevers has been solved by integrating film patterning and deposition with oscillator fabrication. Future work will explore the possibility of decreasing the quantitative error by recording full cantilever resonance sweeps at each value of magnetic field. This will allow for the frequency shift, dissipation, and cantilever deflection all to be measured and used in analysis. Long-term cantilever optimization combined with low temperatures makes this method a promising technique for measuring magnetic properties of individual samples near the superparamagnetic regime of $10\ \text{nm} \times 10\ \text{nm}$.

- ¹X. Zhu, P. Grutter, V. Metlushko, and B. Ilic, *Appl. Phys. Lett.* **80**, 4789 (2002); U. Wiedwald, M. Spasova, M. Farle, M. Hilgendorff, and M. Giersig, *J. Vac. Sci. Technol. A* **19**, 1773 (2001); J. Jorzick, S. O. Demokritov, B. Hillebrands, B. Bartenlian, C. Chappart, D. Decanini, F. Rousseaux, and E. Cambil, *Appl. Phys. Lett.* **75**, 3859 (1999).
- ²M. Lederman, S. Schultz, and M. Ozaki, *Phys. Rev. Lett.* **73**, 1986 (1994).
- ³R. H. Koch, J. G. Deak, D. W. Abraham, P. L. Trouilloud, R. A. Altman, Y. Lu, W. J. Gallagher, R. E. Scheuerlein, K. P. Roche, and S. S. P. Parkin, *Phys. Rev. Lett.* **81**, 4512 (1998); S. E. Russek, S. Kaka, and M. J. Donahue, *J. Appl. Phys.* **87**, 7070 (2000); J. Aumentado and V. Chandrasekhar, *Appl. Phys. Lett.* **74**, 1898 (1999).
- ⁴R. P. Cowburn, D. K. Koltsov, A. O. Adeyeye, and M. E. Welland, *Appl. Phys. Lett.* **73**, 3947 (1998).
- ⁵C. Salling, R. O'Barr, S. Schultz, I. McFadyen, and M. Ozaki, *J. Appl. Phys.* **75**, 7989 (1994).
- ⁶W. Wernsdorfer, D. Mailly, and A. Benoit, *J. Appl. Phys.* **87**, 5094 (2000).
- ⁷B. C. Stipe, H. J. Mamin, T. D. Stowe, T. W. Kenny, and D. Rugar, *Phys. Rev. Lett.* **86**, 2874 (2001).
- ⁸C. Rossel, P. Bauer, D. Zech, J. Hofer, M. Willemin, and H. Keller, *J. Appl. Phys.* **79**, 8166 (1996).
- ⁹J. G. E. Harris, D. D. Awschalom, F. Matsukura, H. Ohno, K. D. Maranowski, and A. C. Gossard, *Appl. Phys. Lett.* **75**, 1140 (1999).
- ¹⁰M. Löhndorf, J. Moreland, P. Kabos, and N. Rizzo, *J. Appl. Phys.* **87**, 5995 (2000).
- ¹¹J. Moreland, P. Kabos, A. Jander, M. Löhndorf, R. McMichael, and C. G. Lee, *Proc. SPIE* **4176**, 84 (2000).
- ¹²M. Löhndorf, J. Moreland, and P. Kabos, *Appl. Phys. Lett.* **76**, 1176 (2000).
- ¹³R. N. Kleinman, G. K. Kaminsky, J. D. Reppey, R. Pindak, and D. J. Bishop, *Rev. Sci. Instrum.* **56**, 2088 (1985).
- ¹⁴M. D. Chabot and J. T. Markert, *Proc. SPIE* **3875**, 104 (1999).
- ¹⁵R. J. Roark and W. C. Young, *Formulas for Stress and Strain* (McGraw-Hill, New York, 1975).